Alexandria Engineering Journal (2020) 59, 4201–4210

HOSTED BY

ELSEVIER

Alexandria University

Alexandria Engineering Journal

www.elsevier.com/locate/aej
www.sciencedirect.com

Incorporation of Cellulose Nanocrystals (CNC) derived from sawdust into polyamide thin-film composite membranes for enhanced water recovery

Amos Adeniyi [a,*], Danae Gonzalez-Ortiz [b], Celine Pochat-Bohatier [b], Opeyemi Oyewo [a], Bruce Sithole [c], Maurice Onyango [a,*]

[a] *Department of Chemical, Metallurgical and Materials Engineering, Tshwane University of Technology, Pretoria 0001, South Africa*
[b] *Institut Européen des Membranes, IEM UMR-5635, Université de Montpellier, ENSCM, CNRS Place Eugène Bataillon, 34095 Montpellier cedex 5, France*
[c] *Biorefinery Industry Development Facility, Council for Scientific & Industrial Research, Natural Resources and the Environment, Durban, South Africa*

Received 17 May 2020; revised 16 June 2020; accepted 20 July 2020
Available online 1 August 2020

KEYWORDS

Sawdust;
Cellulose nanocrystals;
Polyamide membrane;
Interfacial polymerization;
Water flux;
Rejection

Abstract In this work, cellulose nanocrystals (CNC) derived from sawdust were successfully incorporated into a thin film composite membrane made from polyamide. The characteristics of unmodified and modified membranes were investigated using FT-IR, XRD, TGA, SEM, EDX, AFM and contact angle measurement. The membranes' performances were evaluated using a dead-end test cell with sodium chloride (1500 ppm) and calcium chloride (2500 ppm) solutions. FT-IR and XRD analyses revealed that polymerization took place during the incorporation of the cellulose nanocrystals. From EDX analysis, it was found that incorporation of CNC into the membrane resulted in an increase in the oxygen content both at the atomic and mass levels. SEM and AFM images revealed dense and tight structures for both modified and unmodified membranes. The modified membrane was more hydrophilic and rougher than the unmodified membrane. The water flux was significantly increased (more than 23%) while maintaining high rejection rate values for sodium chloride (98.3 ± 0.8%) and calcium chloride (97.1 ± 0.5%). Furthermore, there was also an increase in the thermal stability of the membrane. The results, therefore, have shown a great prospect in the development of thin-film nanocomposite membranes using sawdust-derived cellulose nanocrystals incorporated in polyamide.

1. Introduction

Water is essential to life; however, this important commodity is becoming scarce all over the world [1]. This is because the change in water usage pattern has put a strong demand on

* Corresponding authors.
E-mail addresses: adeniyia@tut.ac.za (A. Adeniyi), OnyangoMS@tut.ac.za (M. Onyango).
Peer review under responsibility of Faculty of Engineering, Alexandria University.

https://doi.org/10.1016/j.aej.2020.07.025

available limited fresh water. For instance, the proliferation of high-tech industries has significantly increased water demand and at the same time resulted in generation of hard-to-treat wastes such as pharmaceutical products, organic wastes, heavy metals and other endocrine disrupting substances. Besides, the world population is growing at an alarming rate and thus creating extra needs for quality drinking water and water for other uses. Thus, as a result of the numerous water quality issues facing humanity today, there is a strong need to improve or develop new and appropriate technologies to treat water.

Membrane technology has been recognized as an effective water treatment tool for contaminant removal from polluted water supplies [2]. The most used driving force for transport in membrane processes is the gradient of pressure. There are essentially four pressure-driven membrane processes that are classified according to the size of the membrane pores and thus the pollutants that can be removed depending on the design of the membrane [3–5]. Tight and non-porous membranes can reject monovalent and divalent ions. However, the pressure required to drive water across the membrane is higher than that of porous membranes. Indeed, the invention of thin film composite (TFC) membranes for water treatment was a major breakthrough in membrane synthesis leading to high flux, monovalent salt rejection, better rejection of organic compounds, and excellent stability in high temperature, in alkaline and acidic environments [6].

TFC membranes are usually made from either polyamide or polyetherurea [7]. Polyamide membranes are cast on an ultrafiltration (UF) membrane as a support in order to give them rigidity and mechanical strength required. The active polyamide thin film layer is responsible for solute removal and water recovery. Several attempts have been made to improve the thin film composite membrane performance and longevity through the incorporation of different materials. The resulting membrane when nanomaterials are incorporated into thin film composite membrane is called thin film nanocomposite (TFN) membrane [8]. TFN membranes are expected to display an improved flux and fouling resistance than thin film composite membranes [9]. Various nanomaterials including carbon nanotubes (CNTs), silica, graphene oxide (GO) and titanium oxide have been used to fabricate thin film nanocomposite membranes resulting in improved fouling resistance, hydrophilicity and perm-selectivity of the membranes [9–13]. Zhao et al [14] recently incorporated UiO-66-NH_2 nanoparticles into thin film composite polyamide membrane. The nanoparticles were deposited on the support substrate using a spray nozzle. Such membranes are usually referred to as TFC with nanocomposite substrate [15]. They reported increase in water flux with a marginal decrease in solute rejection. Zhao et al [16] succeeded in incorporation poly (ethyleneglycol) 200 (PEG200) into thin film composite membrane with the assistance of Laponite as nanofillers. The resulting thin film nanocomposite membrane resulted in improved water flux. Gai et al. [17] recently developed a thin film nanocomposite hollow fibre membrane by incorporating Na^+-functionalized carbon quantum dots (Na-CQDs) into the polyamide layer. They also reported an improvement in water flux without compromising the salt rejection. However, there is an environmental and health concern with the use of membranes having any of these nanomaterials [18,19]. Cellulose nanomaterials provide a suitable alternative to these environmentally hazardous nanomaterials [19–21].

Cellulose nanomaterial is comparable to carbon nanotubes in terms of material properties [19,21]. Similar to carbon nanotubes, incorporation of cellulose nanomaterials into polymer matrix even at a very low weight percent modifies the membrane properties. This leads to increase in membrane hydrophilicity, membrane tensile strength, resistance to fouling, greater permeability and selectivity. Other advantages of cellulose nanomaterials are with regard to biocompatibility and environmental friendly nature [19]. There are several forms of cellulose nanomaterials. The notable ones are cellulose nanocrystals (CNC) and cellulose nanofibrils (CNF) [22,23]. This work focuses on CNC. Industrially, CNC is derived majorly from wood, however, the use of wood as source of natural CNC is an expensive endeavour and thus alternatives must be found.

Sawdust is a waste generated from forestry and timber industry and accounts for over 40% of the wastes [24]. Most of the sawdust waste has not been converted into useful products and ends up being destroyed in landfill sites or by burning [25]. It is imperative therefore to find use of sawdust in the production of cellulose nanocrystals as a cheap alternative raw material. The novelty of this work is to incorporate CNCs derived from a cheap source: sawdust, into thin film polyamide membranes. The comparison of the property of unmodified and modified TFC membranes clearly shows that the incorporation of sawdust-derived cellulose nanocrystals leads to an increase of water filtration fluxes without affecting the rejection of sodium chloride and calcium chloride.

2. Materials and methods

2.1. Material

Analytical grade chemicals used for the study including m-phenylene-diamine (MPDA), trimesoyl chloride (TMC), hexane, sodium dodecyl sulphate, sodium hydroxide, ammonium chloride, sodium chloride and calcium chloride were all obtained from Sigma-Aldrich, South Africa. The cellulose nanocrystals (CNC) used were obtained from CSIR, Durban. Fig. 1 shows TEM image of the CNC in which a mono dispersed dot-like shape with average particle size of 5.98 nm is revealed [26]. The polysulfone UF membrane (100 kDa) used

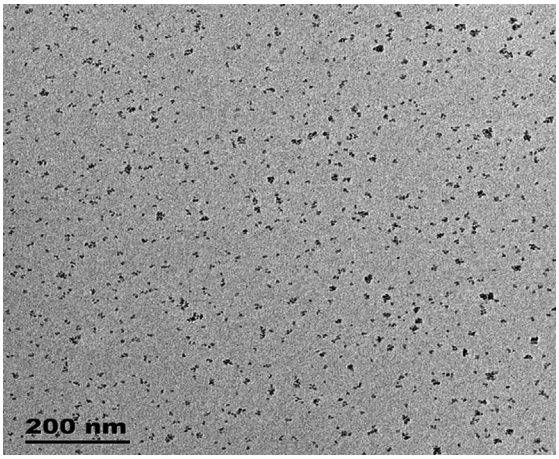

Fig. 1 Transmission electron microscopy (TEM) of the CNCs used in this work [26].

as a support was obtained from Microdyn Nadir. Quality of the deionized water used was between 14 and 15 mΩ and was produced using the Purite water system (Model Select Analyst HP40, United Kingdom).

2.2. Membranes syntheses

Two membranes were synthesised and named PA (unmodified) and PA-CNC (modified). Both membranes were synthesised using interfacial polymerization method. In the preparation of PA, UF polysulfone membrane was soaked into a solution containing 0.5% sodium dodecyl sulphate (SDS) for 12 h. SDS is used to increase the wettability of the substrate so that monomers can easily move from one phase to another [27]. Afterwards, the membrane was washed and drenched in deionized water for 2 h, after which it was dried for 1 h in a fume cupboard. The membrane was then placed with a double-sided tape onto a glass plate. The aqueous solution has meanwhile been prepared by adding 1 g of MPDA to 100 mL of deionized water. 0.4 g sodium hydroxide was added as acid acceptor in order to consume the hydrogen chloride generated in the polymerization reaction which could reduce the reactivity of the monomer reactants in the aqueous phase [28,29]. The pH was adjusted to eight (8) by adding ammonium chloride. The organic solution was prepared by adding 0.5 g Trimesoyl chloride (TMC) to 100 mL of hexane. The aqueous solution was poured on UF membrane and allowed to stay for 30 min. Excess aqueous solution was removed from the membrane by using filter papers to wipe its surface, and the organic solution was then added. The reaction was allowed to proceed for 60 s. The synthesised membrane was allowed to drain and then cured in an oven at 65℃ for 15 min. The prepared membrane was washed and soaked in deionized water. In the case of PA-CNC membrane preparation, the same procedure for the preparation of the PA membrane was used except that 0.21 g of cellulose nanocrystals (CNC) was added to the aqueous solution. 0.21 g of CNC was used because it gave the best result after trial of various masses of CNC. The proposed reaction mechanism and procedure for the incorporation of cellulose nanocrystals during polymerization process are shown in Fig. 2.

2.3. Membrane characterization

The membranes were characterized using Fourier transform infra-red (FT-IR) spectroscopy to determine the functional groups present on the surface. The analysis was done with a Perkin Elmer Spectrum 100 spectrometer, with wavelength recording done in the 500–4000 cm^{-1} range at a resolution of 4 cm^{-1}. The membrane surface and cross-section morphologies were investigated using a Hitachi S4800 scanning electron microscopy system (SEM). For the SEM analysis, the samples were first coated with platinum using an ion sputter coater. The cross section length was measured using ImageJ software [30]. Energy-dispersive X-ray spectroscopy analysis (EDX) was performed with Zeiss EVO ED15 microscope coupled with an Oxford X-MaxN EDX detector. Characterization of the Atomic Force Microscopy (AFM) was performed using Molecular Imaging (FastScan Dimension, Bruker) in tapping mode to describe the thin film surface morphology. Silicon cantilevers (Fastcsan-A) with a typical tip radius of ≈5 nm were used. The cantilevers had a resonance frequency of around 1.25 kHz. The 2D AFM images were taken on a 400 nm scale. The 2D images were converted to 3D images using WSxM 5.0 Develop 9.1 software [31]. A PANalytical Xpert device was used to record X-ray diffraction (XRD) patterns of the PA and PA-CNC membranes. The device was operated with Cu Kα radiation at a scanning speed of 2° min^{-1} and at a step rate of 0.02° per second between 2θ range of 10° and 70°. A thermogravimetric analyser (TA Instruments TGA G500 model) was used to analyze the thermal activity of the prepared membranes from 20 °C to 1000 °C. The heating rate was kept constant at 10 °C/min. The experiment was carried out under N_2 atmosphere and at a flow rate of 60 mL/min. A dry sample weighing about 5 mg was used for each experiment. Goniometer (Digidrop-GBX) was used to measure the contact angle by pendant drop method. The measurements were performed by using ultrapure water. A drop of water was deposited onto the surface using a micro syringe, and the reading was taken 5 s after deposition. Five readings were taken at different locations on the membrane and the average of the values was taken as the contact angle.

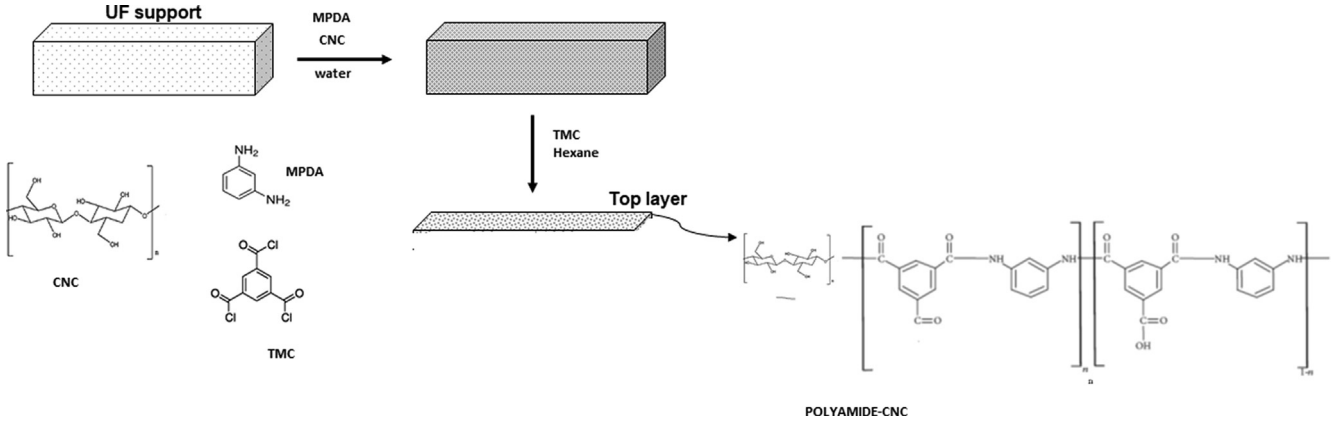

Fig. 2 Procedure for synthesis and suggested mechanism of reaction.

2.4. Water treatment performance tests

The performance tests in terms of water flux, sodium chloride rejection and calcium chloride rejection were done using a dead-end test cell. The membranes were first compacted at a pressure of 5 bar for 8 h. The pure water flux was investigated at pressure ranging from 6 bar to 10 bar. In addition, Sodium Chloride (NaCl) solution (concentration of 1500 ppm) and Calcium Chloride ($CaCl_2$) solution (concentration of 2500 ppm) were treated with the membranes using the test cell at pressure ranging from 6 bar to 10 bar. The conductivity of the feed and final permeate were determined using a conductivity meter. In the test cell, the active membrane area was 14.6 cm^2. Using Eq. (1) the permeate flux was calculated.

$$J_w = \frac{V}{At} \tag{1}$$

where J_w (L/m^2/h) and V (L) are the water flux and the permeate volume respectively. The active membrane area A is measured in m^2 while the filtration time t is in h.

Rejection of the solute was determined using Eq. (2):

$$R = \frac{(C_f - C_p)}{C_f} * 100 \tag{2}$$

where R is the rejection in %, C_f is the solute concentration in the feed and C_p is the solute concentration in the permeate.

3. Results and discussion

3.1. Functional group, phase and elemental composition analyses

FT-IR was used to identify the functional groups present in both membranes. The results of the FT-IR scan for the raw CNC, unmodified membrane (PA) and modified membrane (PA-CNC) are shown in Fig. 3. The peak at 1820–1650 cm^{-1} assigned to C═O band of the amide I group is observed in both membranes indicating that polymerization took place. These peaks appear at 1743 cm^{-1} for the unmodified membrane and at 1670 cm^{-1} for the modified membrane. The fact that polymerization took place is further evidenced in the band 1600–1450 cm^{-1} that is characteristic of amide II [32]. C—N stretch and aromatic ring breathing peaks were observed in both membranes [33]. They appear at 1490 and 1590 cm^{-1} for the modified membrane and at 1463 cm^{-1} and 1473 cm^{-1} for the unmodified membrane. The band at 3000–2850 cm^{-1} which is assigned to sp^3 hybridized C—H bonds, is observed for polyamide membrane and for polyamide membrane containing the CNC. The bands appear at 2844 cm^{-1} and 2916 cm^{-1} for modified membrane and at 2848 cm^{-1} and 2917 cm^{-1} for the unmodified membrane. These show that the thin film was properly formed for both the modified and the unmodified membrane. Polymerization of monomers such as MPDA and TMC always give high degree of crosslinking leading to rejection of both monovalent and divalent ions [34]. The implication is that both membranes can effectively reject monovalent and divalent ions. The band at 3550–3200 cm^{-1} which is assigned to —O—H group was observed on both the raw CNC and modified membranes. This is an evidence of the presence of the CNC in the membrane. The peak was 3340 cm^{-1} for both the raw CNC and the modified membrane but was not observed on the unmodified membrane. This implies that the modified membrane is expected to be more hydrophilic with lower contact angle and increased water flux because of the additional —O—H group from the CNC.

The XRD patterns of both the modified and unmodified membranes are shown in Fig. 4. Besides the peaks that are common to both membranes, there appear in the modified membrane, peaks at 2θ: 16.5°, 18° and 25°. These peaks are assigned to cellulose in different forms [35,36]. This is an evidence of successful incorporation of cellulose nanocrystals into the polyamide membrane. EDX results also revealed an increase in oxygen contents in the modified membrane based on mass and atomic composition. For the modified membrane,

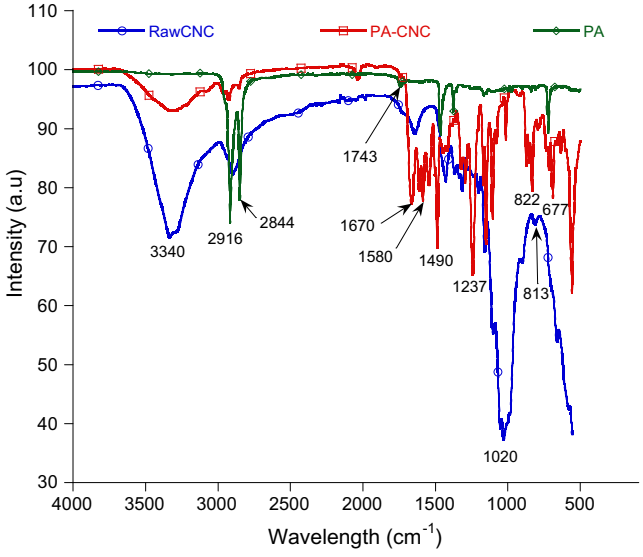

Fig. 3 FT-IR scans of the raw CNC, unmodified membrane (PA) and modified membrane (PA-CNC).

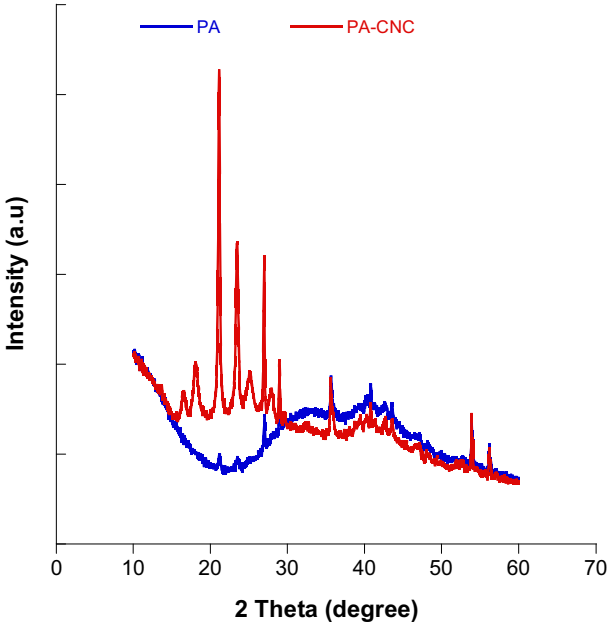

Fig. 4 XRD patterns of unmodified membrane (PA) and the modified membrane (PA-CNC).

percentage mass of oxygen was 16% while that of unmodified was 14%. In terms of atomic composition, oxygen was 13% for the modified against 11% for the unmodified membrane. This can be explained by the addition of —OH group from the cellulose nanocrystals to the polyamide. This is also expected to result in lower contact angle and consequently higher water flux from the CNC modified membrane.

3.2. Membrane morphology

Fig. 5 shows the SEM images on different scales and magnification for a detailed examination of the morphology of the membrane surface and cross section. The images of both modified and unmodified membranes (Fig. 5a–d) reveal uniform and non-porous structure. Some voids were observed on the membranes; these were seen clearly by scanning those spots at lower scales and higher magnifications. The voids were more pronounced on the modified membrane; this may be due to the re-arrangement of the polyamide film as a result of the modification [37].

Smith et al. [38] has proposed a mechanism for the incorporation of nanoparticles in polyamide membranes. It is based on the disrupted bond formation between the monomers and the crosslinking agents that leads to the formation of voids in the resulting polymer matrix as alternative water molecule transport pathways. Such voids are wide enough to allow water

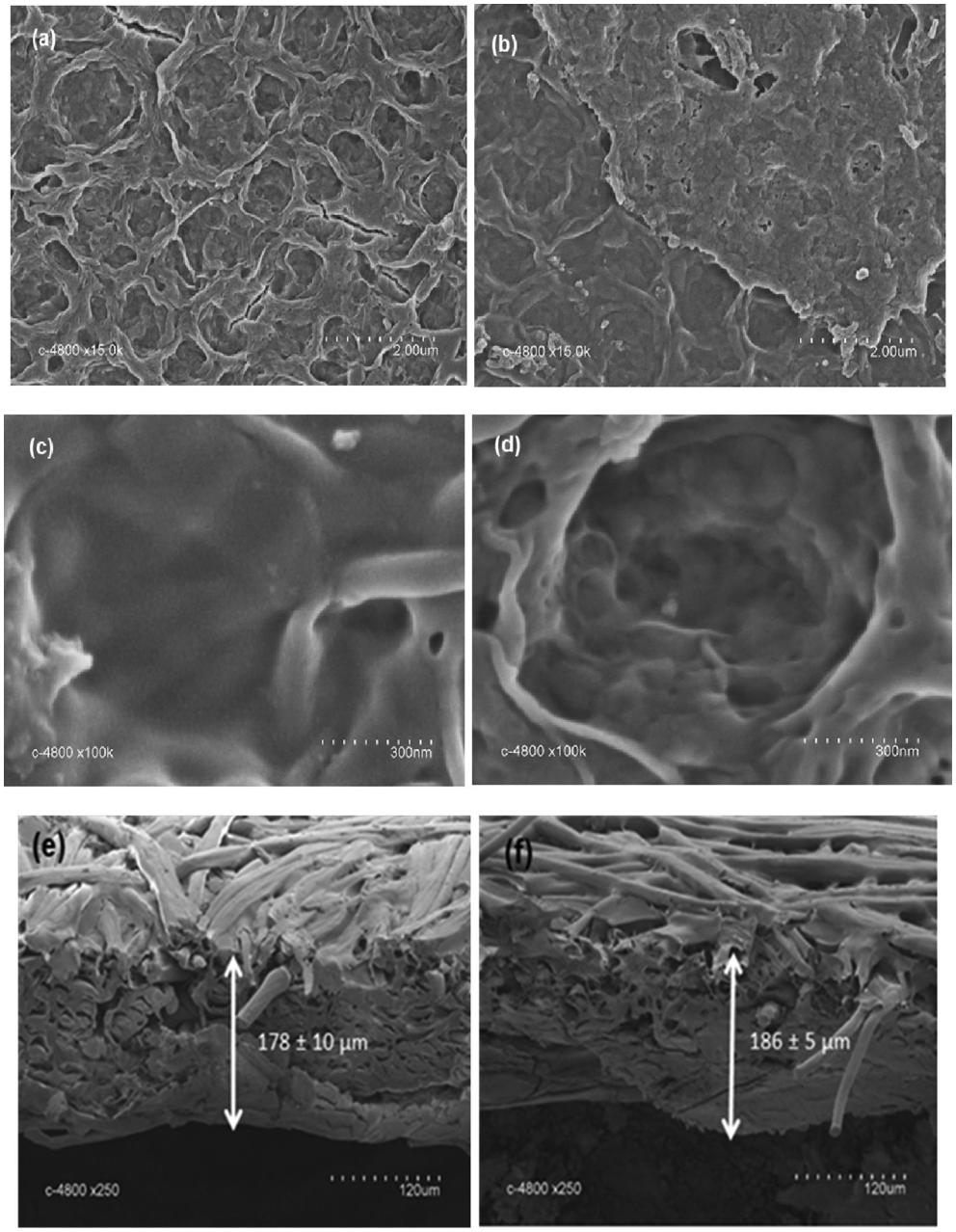

Fig. 5 SEM images of unmodified and modified polyamide membrane at different magnifications (a, c, e) unmodified membrane (b, d, f) modified membrane. (e) and (f) are cross section for unmodified and modified membranes, respectively.

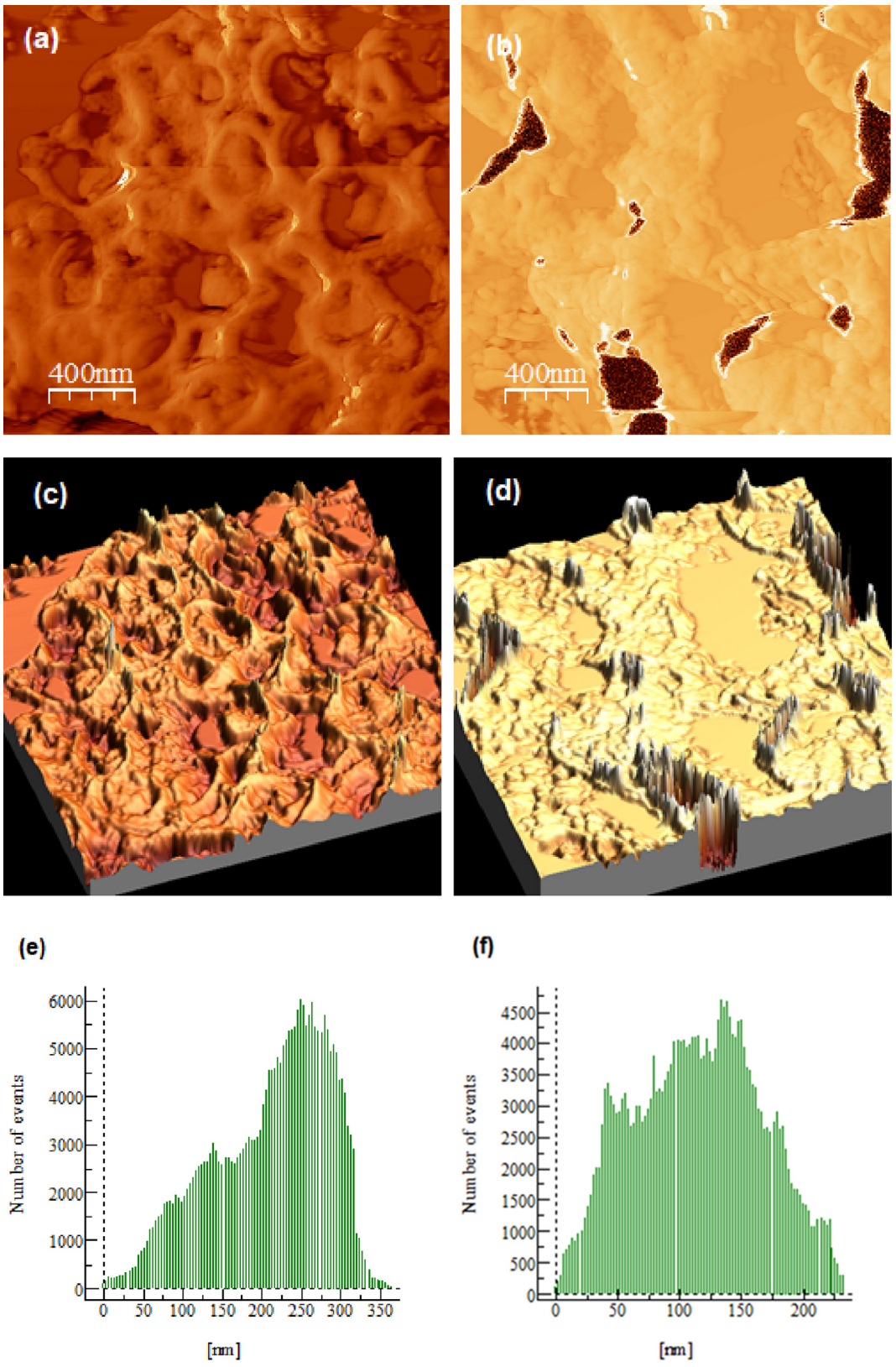

Fig. 6 AFM images and roughness analysis of unmodified and modified polyamide membrane at different magnifications (a) 2D image of unmodified membrane (b) 2D image of the modified membrane (c) 3D image of the unmodified membrane (d) 3D image of the modified membrane (e) Roughness analysis of the unmodified membrane (f) Roughness analysis of the modified membrane.

molecules to move through but small enough to reject all sodium and chloride ions. This interrupt is also suggested by the FT-IR of the modified membrane showing the presence of —OH groups at the same region as that of the raw CNC. The cross-section of both unmodified and modified membranes are shown in Fig. 5e and 5f. The thickness of each membrane was measured using ImageJ software. The figures show that there is a little difference in the thickness of the two membranes. The modified membrane is slightly thicker than the unmodified membrane. This may be because of the attachment of the cellulose nanocrystals to the polyamide film.

The AFM images and the surface roughness analysis of each of the membranes are shown in Fig. 6. The AFM images confirmed that both membranes are non-porous and dense. This means that the degree of crosslinking was high even for the modified membrane despite the incorporation of cellulose nanocrystals. This further explains the reason why both membranes can reject monovalent and divalent ions. The roughness average (R_{avg}) and the root mean square (RMS) roughness (R_{rms}) are two of the most quoted parameters for membrane surface topographies. The roughness average is the arithmetic mean of the surface height (peaks and valleys) deviations with reference to the mean plane of the image. The RMS roughness is the standard deviation of the pixel height data, that is, the deviation of the peaks and valleys from the mean plane. R_{rms} and R_{avg} for the modified membrane were 73.6 nm and 61.2 nm, respectively. For the unmodified membrane, R_{rms} was 61.8 nm while R_{avg} was 43.2 nm (Table 1). These values are useful for the comparison of membrane roughness [39]. The values show that the modified membrane is rougher than the unmodified membrane. The rougher membrane has more ridges and valleys which provides space for more contact with the water drops leading to an increase in water flux [40]. The contact angles of both membranes are also shown in Table 1. The results show that both membranes are hydrophilic but the polyamide membrane incorporated with cellulose nanocrystals was more hydrophilic. This is likely due to the —OH groups present in the CNC modified membrane as shown FT-IR results [41]. A correlation exists between the roughness of the membranes and the hydrophilicity. The unmodified membrane with lower roughness presents higher contact angle while the rougher CNC modified membrane has lower contact angle and thus higher hydrophilicity.

3.3. Thermal gravimetric analysis (TGA)

Both membranes display same pattern of thermal degradation because of the chemical structure of the polyamide mebranes as a result of the presence of amide and benzene rings which are known to be resistant to temperature change [32,42]. However, the modified membrane exhibits better thermal stability as shown in Fig. 7. The first stage of degradation for both polyamide membranes occurred between 304 °C and 551 °C as a result of the splitting of -SO_3H groups from the polysulfone [32]. However, the degradation did not start until a temperature of 466℃ is reached for the CNC modified membrane against 373℃ needed for the unmodified polyamide membrane. This may be due to the incorporation of cellulose nanocrystals [36]. For the unmodified membrane, the first weight loss occurred between the temperature of 373 ℃ and 495 ℃. The second stage of weight drop occurred between the temperature of 495 ℃ and 1000 ℃. For the modified membrane the first weight loss was exhibited between the temperature of 466 ℃ and 499 ℃. The second weight loss occurred between the temperature of 499 ℃ and 1000 ℃. The first weight loss is due to the splitting of the sulfonic group from the polysulfone support while the second degradation is due to breaking down of the cross link in the polyamide membrane [32,43]. This means the membranes are stable at high temperature and can therefore withstand high temperature operations.

Table 1 Roughness parameters and contact angles of the membranes.

Membrane	Roughness parameters (nm)		Contact angle ()
	RMS	R_a	
Unmodified membrane	61.8	43.2	58.3 ± 6.7
Modified membrane	73.6	61.2	36.3 ± 9.8

3.4. Membrane performance

Fig. 8a shows the membranes performance in terms of pure water flux against applied pressure. Eq. (1) was used to calculate the water flux. It is observed that incorporation of cellulose nanocrystals into the PA membrane significantly improves the pure water flux. This may be as a result of increase in hydrophilicity of the modified membrane due to addition of OH group to the polyamide film. Fig. 8b shows the sodium chloride rejection and water flux, when sodium chloride solutions (1500 ppm) was treated. Fig. 8c meanwhile shows the calcium chloride rejection and water flux when a solution of calcium chloride solution (2500 ppm) was treated. The solute rejection was calculated using Eq. (2). In all cases, a significant improvement of water flux was achieved for the modified membrane. The increase in water flux was observed despite the fact that the modified membrane was slightly thicker as shown in Fig. 5 e and f. This is attributed to the presence of the CNC leading to increase in the hydrophilicity and

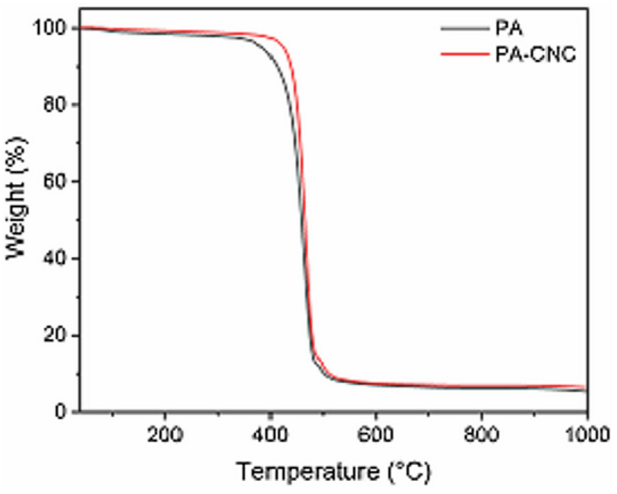

Fig. 7 TGA of unmodified and cellulose nanocrystals modified polyamide membranes.

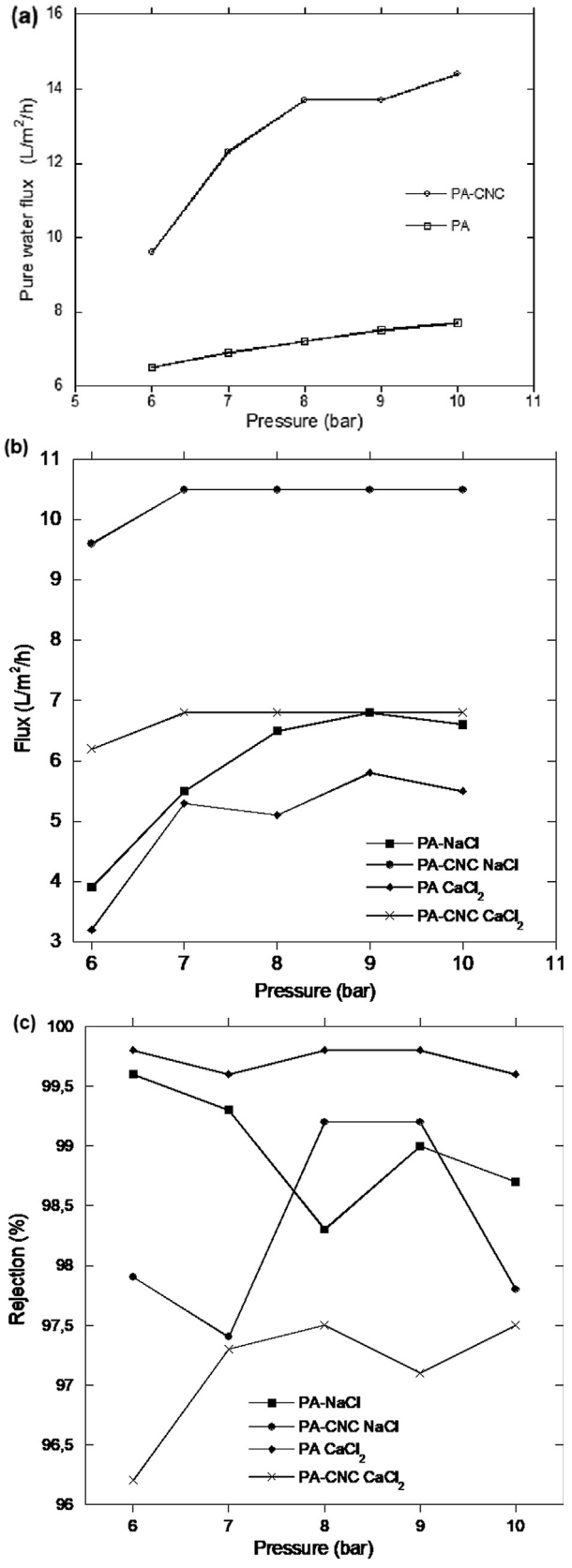

Fig. 8 (a) Pure water flux for the modified and unmodified polyamide membrane (b) water flux when $CaCl_2$ solution and NaCl solution were treated with both the modified and unmodified polyamide membrane; (c) $CaCl_2$rejection and NaCl rejection for both the modified membrane and the unmodified membrane.

Table 2 Comparison of the water flux with other modified polyamide membranes.

Membrane	Water flux (L/m^2/h/bar)	Reference
0.21% sawdust derived CNC modified polyamide	1.44	This study
0.1% CNC modified polyamide	0.43	Smith et al. [38]
βCDTFC(2DA) modified polyamide	0.59	Mbuli et al. [39]
MWCNT modified polyamide	0.88	Park et al. [45]

roughness in the modified membrane. Increase in hydrophilicity leads to an increase in the interaction between the active membrane layer and water causing increase in the water passage [44]. Contact angle for the unmodified membrane was 58.3° ± 6.7°. For the modified membrane the contact angle was 36.3° ± 9.8°; this indicates a higher hydrophilicity than the unmodified membrane. The cellulose nanocrystal increases the density of —OH group on the polyamide membrane leading to an increase in the hydrophilicity of the membrane [36]. Average pure water flux for the modified membrane was 12.7 ± 1.9 L/m^2/h and 7.2 ± 0.5 L/m^2/h for the unmodified membrane. For the $CaCl_2$solution the water flux for the modified membrane was 6.7 ± 0.3 L/m^2/h against 5.0 ± 1.0 L/m^2/h for the unmodified. For the NaCl solution, the average water flux for the modified membrane was 10.3 ± 0.4 L/m^2/h while that of unmodified was 5.9 ± 1.2 L/m^2/h. A minimum of 23% increase in water flux was obtained through the incorporation of the cellulose nanocrystals. The comparison of the water flux obtained for the modified CNC membrane with other membranes in the literature is shown in Table 2. For easy comparison the water flux is expressed as L/m^2/h/bar as the operating pressures were different. Indications are that the membrane developed is this study has a competitively higher flux. Care should be taken though in comparing the materials as different fabrication and testing conditions are employed in these studies.

Fig. 8c shows that there is no significant diference between the rejection of $CaCl_2$ and NaCl for both the modified and unmodified membrane. Average rejection of NaCl for the modified membrane is 98.3 ± 0.8% against 99.0 ± 0.5% for the unmodified membrane. Average rejection of $CaCl_2$ is 97.1 ± 0.5% for the modified membrane while for unmodified was 99.7 ± 0.1%. The high rejection of $CaCl_2$ and NaCl is an evidence that the thin film was properly formed and the membrane is tight and non porous despite the incorporation of cellulose nanocrystals. The results emphasised that the incorporation of CNC into the polyamide membrane increases the water flux while maintaining high $CaCl_2$ and NaCl rejection.

4. Conclusion

In this work, polyamide membrane was succesfully modified by incorporation of the cellulose nanocrystals (CNC) obtained from sawdust using interfacial polymerization technique. The CNC was added to the aqueous phase containing MPDA as monomer. The organic phase contained TMC as the mono-

mer. The CNC modified membrane was compared with the unmodified in terms of characteristics and performances. The characteristics of each membrane were examined using FTIR, XRD, SEM, EDX, AFM, contact angle measurement, and TGA. FTIR, XRD and EDX results confirmed that polymerization took place. SEM images showed that both images are dense and no pores were observed at various magnifications. However, the modified membrane showed a rougher surface than the unmodified. Also, the hydrophilicity of the modified membrane was higher than the value for the unmodified membrane. These lead to higher water flux with the modified membrane. The rejections of $CaCl_2$ and NaCl were higher than 97% for the modified membrane. Both membranes showed good thermal stability but the modified membrane was more thermally stable than the unmodified membrane. These results indicate that the incorporation of sawdust-derived cellulose nanocrystals is a promising method for improving membrane filtration performance while maintaining high salt rejection rates.

Declaration of Competing Interest

The authors declare that they have no known competing financial interests or personal relationships that could have appeared to influence the work reported in this paper.

Acknowledgements

Tshwane University of Technology is acknowledged for providing facilities for the synthesis of the membranes. European Institute of Membrane, University of Montpellier, is acknowledged for providing the facilities for characterization of the membranes. CSIR Durban is acknowledged for the supply of the cellulose nanocrystals. This research has been sponsored by funding from the National Research Foundation (NRF) and the Science and Technology Department (DST), South Africa. The financial support is highly appreciated.

References

[1] M. Abdullahi, D. Machido, Heavy metals resistance potential of some Aspergillus spp. isolated from Tannery wastewater, Nigerian J. Basic Appl. Sci. 25 (2017) 120–129.
[2] S. Sharma, A. Bhattacharya, Drinking water contamination and treatment techniques, Appl. Water Sci. 7 (2017) 1043–1067.
[3] M.K. Selatile, S.S. Ray, V. Ojijo, R. Sadiku, Recent developments in polymeric electrospun nanofibrous membranes for seawater desalination, RSC Adv. 8 (2018) 37915–37938.
[4] D.M. Warsinger, S. Chakraborty, E.W. Tow, M.H. Plumlee, C. Bellona, S. Loutatidou, L. Karimi, A.M. Mikelonis, A. Achilli, A. Ghassemi, A review of polymeric membranes and processes for potable water reuse, Prog. Polym. Sci. 81 (2018) 209–237.
[5] N.A. Ahmad, P.S. Goh, Z. Abdul Karim, A.F. Ismail, Thin film composite membrane for oily waste water treatment: Recent advances and challenges, Membranes 8 (2018) 86.
[6] G.-R. Xu, J.-N. Wang, C.-J. Li, Strategies for improving the performance of the polyamide thin film composite (PA-TFC) reverse osmosis (RO) membranes: Surface modifications and nanoparticles incorporations, Desalination 328 (2013) 83–100.
[7] N. Le, P. Duong, S. Nunes, 1.6 Advanced Polymeric and Organic-Inorganic Membranes for Pressure-Driven Processes, Comprehensive Membrane Sci. Eng. 10 (2017) 120.
[8] W. Lau, S. Gray, T. Matsuura, D. Emadzadeh, J.P. Chen, A. Ismail, A review on polyamide thin film nanocomposite (TFN) membranes: history, applications, challenges and approaches, Water Res. 80 (2015) 306–324.
[9] B.-H. Jeong, E.M. Hoek, Y. Yan, A. Subramani, X. Huang, G. Hurwitz, A.K. Ghosh, A. Jawor, Interfacial polymerization of thin film nanocomposites: a new concept for reverse osmosis membranes, J. Membr. Sci. 294 (2007) 1–7.
[10] R.-X. Zhang, L. Braeken, P. Luis, X.-L. Wang, B. Van der Bruggen, Novel binding procedure of TiO2 nanoparticles to thin film composite membranes via self-polymerized polydopamine, J. Membr. Sci. 437 (2013) 179–188.
[11] V. Vatanpour, M. Safarpour, A. Khataee, H. Zarrabi, M.E. Yekavalangi, M. Kavian, A thin film nanocomposite reverse osmosis membrane containing amine-functionalized carbon nanotubes, Sep. Purif. Technol. 184 (2017) 135–143.
[12] K. Goh, L. Setiawan, L. Wei, R. Si, A.G. Fane, R. Wang, Y. Chen, Graphene oxide as effective selective barriers on a hollow fiber membrane for water treatment process, J. Membr. Sci. 474 (2015) 244–253.
[13] C. Liu, A.F. Faria, J. Ma, M. Elimelech, Mitigation of biofilm development on thin-film composite membranes functionalized with zwitterionic polymers and silver nanoparticles, Environ. Sci. Technol. 51 (2016) 182–191.
[14] D.L. Zhao, W.S. Yeung, Q. Zhao, T.-S. Chung, Thin-film nanocomposite membranes incorporated with UiO-66-NH2 nanoparticles for brackish water and seawater desalination, J. Membr. Sci. 118039 (2020).
[15] J. Yin, B. Deng, Polymer-matrix nanocomposite membranes for water treatment, J. Membr. Sci. 479 (2015) 256–275.
[16] Q. Zhao, D.L. Zhao, T.S. Chung, Nanoclays-Incorporated Thin-Film Nanocomposite Membranes for Reverse Osmosis Desalination, Adv. Mater. Interfaces 7 (2020) 1902108.
[17] W. Gai, D.L. Zhao, T.-S. Chung, Thin film nanocomposite hollow fiber membranes comprising Na + -functionalized carbon quantum dots for brackish water desalination, Water Res. 154 (2019) 54–61.
[18] L. Bai, H. Liang, J. Crittenden, F. Qu, A. Ding, J. Ma, X. Du, S. Guo, G. Li, Surface modification of UF membranes with functionalized MWCNTs to control membrane fouling by NOM fractions, J. Membr. Sci. 492 (2015) 400–411.
[19] A.W. Carpenter, C.-F. de Lannoy, M.R. Wiesner, Cellulose nanomaterials in water treatment technologies, Environ. Sci. Technol. 49 (2015) 5277–5287.
[20] D. Klemm, D. Schumann, F. Kramer, N. Heßler, M. Hornung, H.-P. Schmauder, S. Marsch, Nanocelluloses as innovative polymers in research and application, in: Polysaccharides Ii, Springer, 2006, pp. 49–96.
[21] F. Jiang, Y.-L. Hsieh, Chemically and mechanically isolated nanocellulose and their self-assembled structures, Carbohydr. Polym. 95 (2013) 32–40.
[22] A. Dufresne, Cellulose nanomaterial reinforced polymer nanocomposites, Curr. Opin. Colloid Interface Sci. 29 (2017) 1–8.
[23] H. Kargarzadeh, M. Mariano, D. Gopakumar, I. Ahmad, S. Thomas, A. Dufresne, J. Huang, N. Lin, Advances in cellulose nanomaterials, Cellulose 25 (2018) 2151–2189.
[24] P. Akhator, A. Obanor, A. Ugege, Nigerian Wood Waste: A potential resource for economic development, J. Appl. Sci. Environ. Manage. 21 (2017) 246–251.
[25] A. Demirbas, Waste management, waste resource facilities and waste conversion processes, Energy Convers. Manage. 52 (2011) 1280–1287.
[26] O.A. Oyewo, B. Mutesse, T.Y. Leswifi, M.S. Onyango, Highly efficient removal of nickel and cadmium from water using sawdust-derived cellulose nanocrystals, J. Environ. Chem. Eng. 7 (2019) 103251.

[27] W. Lau, A. Ismail, N. Misdan, M. Kassim, A recent progress in thin film composite membrane: a review, Desalination 287 (2012) 190–199.
[28] M.J. Raaijmakers, N.E. Benes, Current trends in interfacial polymerization chemistry, Prog. Polym. Sci. 63 (2016) 86–142.
[29] J. Gohil, A.K. Suresh, Performance and Structure of Thin Film Composite Reverse Osmosis Membranes Prepared by Interfacial Polymerization in the Presence of Acid Acceptor, J. Membrane Sci. Res. 5 (2019) 3–10.
[30] A. Adeniyi, R. Mbaya, M. Onyango, M. Sethoga, V. Hlongwane, J. Mosesane, O. Olukunle, J. Maree, Water recovery and rejection of organochloride pesticides during reverse osmosis process, J. Comput. Theor. Nanosci. 14 (2017) 5103–5109.
[31] I. Horcas, R. Fernández, J. Gomez-Rodriguez, J. Colchero, J. Gómez-Herrero, A. Baro, WSXM: a software for scanning probe microscopy and a tool for nanotechnology, Rev. Sci. Instrum. 78 (2007) 013705.
[32] M.M. Said, A.H.M. El-Aassar, Y.H. Kotp, H.A. Shawky, M.S. A. Mottaleb, Performance assessment of prepared polyamide thin film composite membrane for desalination of saline groundwater at Mersa Alam-Ras Banas, Red Sea Coast, Egypt, Desalination and Water Treatment 51 (2013) 4927–4937.
[33] P.S. Singh, S. Joshi, J. Trivedi, C. Devmurari, A.P. Rao, P. Ghosh, Probing the structural variations of thin film composite RO membranes obtained by coating polyamide over polysulfone membranes of different pore dimensions, J. Membr. Sci. 278 (2006) 19–25.
[34] F.A.A. Ali, J. Alam, A.K. Shukla, M. Alhoshan, B.M.A. Abdo, W.A. Al-Masry, A Novel Approach to Optimize the Fabrication Conditions of Thin Film Composite RO Membranes Using Multi-Objective Genetic Algorithm II, Polymers 12 (2020) 494.
[35] A.D. French, Idealized powder diffraction patterns for cellulose polymorphs, Cellulose 21 (2014) 885–896.
[36] J. Gong, J. Li, J. Xu, Z. Xiang, L. Mo, Research on cellulose nanocrystals produced from cellulose sources with various polymorphs, RSC Adv. 7 (2017) 33486–33493.
[37] B.S. Mbuli, E.N. Nxumalo, R.W. Krause, V.L. Pillay, Y. Oren, C. Linder, B.B. Mamba, Modification of polyamide thin-film composite membranes with amino-cyclodextrins and diethylamino-cyclodextrins for water desalination, Sep. Purif. Technol. 120 (2013) 328–340.
[38] E.D. Smith, K.D. Hendren, J.V. Haag, E.J. Foster, S.M. Martin, Functionalized Cellulose Nanocrystal Nanocomposite Membranes with Controlled Interfacial Transport for Improved Reverse Osmosis Performance, Nanomaterials 9 (2019) 125.
[39] B.S. Mbuli, E.N. Nxumalo, S.D. Mhlanga, R.W. Krause, V.L. Pillay, Y. Oren, C. Linder, B.B. Mamba, Development of antifouling polyamide thin-film composite membranes modified with amino-cyclodextrins and diethylamino-cyclodextrins for water treatment, J. Appl. Polym. Sci. 131 (2014).
[40] A. Adeniyi, M. Onyango, M. Bopape, Impact of nodular structure in characterization of three thin film composite membranes made from 1, 2-benzisothiazol-3 (2H)-one, sodium salt, (2019).
[41] Z. Yang, Y. Zhou, Z. Feng, X. Rui, T. Zhang, Z. Zhang, A review on reverse osmosis and nanofiltration membranes for water purification, Polymers 11 (2019) 1252.
[42] J.A. Reglero Ruiz, M. Trigo-López, F.C. García, J.M. García, Functional aromatic polyamides, Polymers 9 (2017) 414.
[43] A. Al-Hobaib, M. Alsuhybani, K.M. Al-Sheetan, Reverse osmosis membrane modified by interfacial polymerization in non-polar heptane solvent assistance with acetone as a co-solvent, Water Resour. Manage. 8 (2015) 245.
[44] F. Xu, M. Wei, X. Zhang, Y. Song, W. Zhou, Y. Wang, How Pore Hydrophilicity Influences Water Permeability?, Research 2019 (2019) 2581241.
[45] J. Park, W. Choi, S.H. Kim, B.H. Chun, J. Bang, K.B. Lee, Enhancement of chlorine resistance in carbon nanotube based nanocomposite reverse osmosis membranes, Desalin. Water Treat. 15 (2010) 198–204.